THE JOURNAL OF PHYSICAL CHEMISTRY B

Article

pubs.acs.org/JPCB

Amino Acid Tautomerization Reactions in Aqueous Solution via Concerted and Assisted Mechanisms Using Free Energy Curves from MD Simulation

Santiago Tolosa,* Antonio Hidalgo, and Jorge A. Sansón

Departamento de Ingeniería Química y Química Física, Universidad de Extremadura, 06071-Badajoz, Spain

ABSTRACT: A theoretical study is described of chemical reactions in solution by means of molecular dynamics simulations, with solute−solvent interaction potentials derived from AMBER van der Waals parameters and QM/MM electrostatic charges in solution. The solvent is used as the reaction coordinate, and the free energy curves to calculate the properties related to the reaction mechanism. The proposed scheme is applied to the tautomerization process in aqueous solution for some amino acids $H_2NCHR-COOH$ (with R = H being glycine, R = CH_3 alanine, R = CH_2OH serine, and R = CH_2COOH aspartic acid), focusing on the role of the solvent in the reaction (assisted versus unassisted mechanisms) and on the effect of the hydrophilic/hydrophobic character of the radical R on the activation and reaction energies.

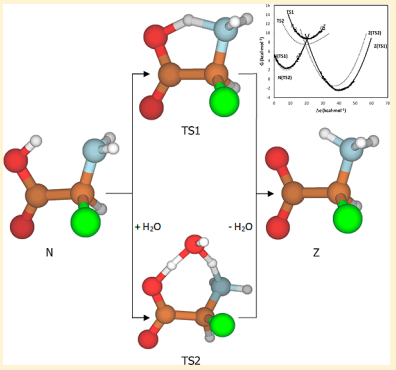

1. INTRODUCTION

There has been growing theoretical interest in studying processes in solution such as the tautomerization of amino acids.[1−18] We shall here describe a computational study of the role of the solvent and substituent effects on amino acid tautomerization. Although tautomerization of amino acids between the neutral form (N) and the zwitterionic form (Z) in water has been widely studied, often using glycine as a model, the process remains poorly understood because of the many different aspects involved in the reaction. An appropriate description of isomerization processes requires an effective model to describe the charge, the adequate solvation structure, and the right choice of reaction pathways.

One of the main difficulties in this type of study is the great number of atoms present and, hence, of the molecular interactions that occur. A complete quantum-mechanical treatment is thus too costly, and approximate methods have to be applied. This is not the only difficulty that has to be faced in the case of chemical reactivity in solution, however, since one has to take into account the possibility that the solvent participates in the chemical reaction. Therefore, the reaction does not have to follow a concerted mechanism passing through a single saddle point, but can take place in various stages (a stepwise mechanism) or in a single stage with participation of the solvent (assisted-concerted mechanism).

There exist various procedures for the study of chemical systems in solution. Examples are those that include the effect of the solvent as a dielectric (the polarizable continuum model, PCM[19]), that use a quantum/classical computational model (QM/MM[20]), or that make a complete quantum-mechanical treatment of the system (CP[21]) using molecular dynamics (MD[22]). Our research group has been using the classical method of molecular dynamics to simulate chemical processes and systems in dilute aqueous solutions. In this, we describe the solute−solvent interaction through simple analytical functions whose molecular parameters are obtained by fitting ab initio calculations of the interaction energies or by using of the most commonly used potentials, e.g., the AMBER,[23] OPLS,[24] CHARM,[25] GROMOS,[26] and MM3[27] force fields for the solute. To describe the water−water interaction, we use the TIP3P[28] potential. We then proceed to simulate the system using one of the statistical methods of molecular mechanics—the MD/MM method. In this context, it becomes feasible to study the properties related to the reaction process, especially with respect to determining the free energies of the systems involved in these processes. The MD/MM method also allows the free-energy curves of the species involved in the reaction to be constructed on the basis of the fluctuation of the solute−solvent interaction energy. The result is to provide values for the properties associated with the chemical reactivity (reaction energies, activation barriers, rate constants, equilibrium constants, etc.) without having to know the exact path the chemical reaction takes.

The objective of the present work was to describe the geometry and thermodynamics of the tautomerization reaction of amino acids in aqueous solution. We shall also present energy values for these reactions, which should be of particular interest considering that there are very few results published for the amino acids we shall be considering except for glycine and the results have often been contradictory. The treatment of the concerted mechanisms, nonassisted and assisted, includes an analysis of the effect of the solvent on the reaction and

Received: July 26, 2012
Revised: October 9, 2012
Published: October 17, 2012

dx.doi.org/10.1021/jp307391s | J. Phys. Chem. B 2012, 116, 13033−13044

activation free energies. Other objectives were to examine the role of the hydrophilic or hydrophobic character of the radical −R in modifying the barrier and reaction energy, and to search the transition states for the different processes in solution under study. The analysis is made not only as a function of the free energy curves, but also considering the solute−solvent interaction contour maps and the radial distribution functions of the atoms involved in the proton transfer. All these calculations were carried out for the first time with a modification of our procedure[29−40] which will be detailed in section 3, including the ASEP charges[41] from QM/MM calculations to describe the electrostatic part and the AMBER parameters[23] to describe the van der Waals components.

2. THE AMINO ACIDS AND MECHANISMS STUDIED

The tautomeric equilibrium of glycine, the smallest amino acid, is of prime importance since it can be considered as a model for the study of this reaction for other amino acids. While in the gas phase the neutral form (N) is the most stable, in aqueous solution the zwitterionic (Z) form is stabilized by electrostatic interactions between the aqueous solvent and the amino acid, leading to tautomeric processes that are faster and slightly exothermic.

Quantum-chemical calculations are today a powerful theoretical tool with which to complement experimental data, or even replace them in experimentally difficult situations. For example, many theoretical and experimental methods have been applied to studying the tautomeric equilibrium of glycine, among them, the thermodynamic[42−44] and chemical relaxation[45] experimental measurements, and the FEP/MD,[46] DF/MD,[47] HF,MP2,DFT/PCM,[48−50] ReaxFF/MD,[51] DFT/supermolecule,[52,53] QM/MM/PCM,[54,55] and AIMD[56] theoretical methods. While the experimental results give an activation barrier $\Delta G^{\#}$ about 7 kcal·mol^{-1} and a reaction energy value ΔG_R between −7.3 and −7.7 kcal·mol^{-1} for the N → Z process, the theoretical results change drastically depending on the procedure used. Thus, while Nagaoka et al.[46] obtained values of $\Delta G^{\#}$ = 8.5 and ΔG_R = −8.4 kcal·mol^{-1}, in very good agreement with experimental results; Tuñon et al.[50] obtained values of $\Delta G^{\#}$ = 0.6 and ΔG_R = −4.7 kcal·mol^{-1} far from the experimental results. Similarly, Tortonda et al.[48,49] obtained different energies depending of the level and number of water molecules considered ($\Delta G^{\#}$ = 2.39 and ΔG_R = −1.15 kcal·mol^{-1} for the MP2/PCM calculation using only the continuum model). In the latter of these two works, it was shown that the barrier is lower when the reference state is separate glycine + H_2O instead of glycine-H_2O complex. A more recent work of Rahaman et al.,[51] using a reactive force field (ReaxFF) and molecular dynamics simulation, finds that the assisted mechanism may be preferred over the nonassisted in terms of enthalpy, but that the entropy correction may modify this conclusions. They report that the nonassisted mechanism activation barrier is somewhat higher than the experimental value, but the reaction energy is in good agreement with experiment. Balta and Aviyente,[52,53] using a DFT method and six water molecules to study the enthalpy and entropy components in the activation and reaction energy, find a greater contribution of the enthalpy in contradiction with experiment,[45] and a favorable tautomerization process only when a large number of solvent molecules are considered. Recent studies using QM/MM models obtain very different values for the reaction energy. Shoeib et al.[54] report a highly exothermic value, but Cui[55] gets a good value of −7.0 kcal·mol^{-1}, and Leung et al.[56] of −11.2 kcal·mol^{-1}.

The studies of the tautomerization of alanine, the most abundant amino acid in proteins, are few in number. Tortonda et al.,[49] using the DF/PCM method, obtain a result similar to that for glycine, but with more stable TS y Z structures due to $-CH_3$ group. In particular, the activation barriers are between 2 and 11 kcal·mol^{-1} and the reaction energies between −0.5 and −3.6 kcal·mol^{-1}. Sambrano et al.,[57] using the HF,MP2/SCRF method, obtain a zwitterionic structure that is more stable than the neutral only when the electronic correlation is considered, with an activation barrier $\Delta E^{\#}$ = 2.2 and a reaction energy ΔE_R = −3.6 kcal·mol^{-1} at the MP2/SCRF level of calculation. Park et al.,[58] studying alanine taumerization at the MP2/6-31++G** level and considering several solvent molecules participating in the reaction mechanism, find barriers $\Delta E^{\#}$ ranging from 1.8 to 2.6 kcal·mol^{-1}, depending on the number of protons transferred. Finally, Gontrani et al.[59] study the effect of solvent on the tautomerization energy of glycine and alanine with the PCM model, finding surprisingly that the process is slightly more favorable for alanine (ΔG_R = −4.9 kcal·mol^{-1}).

The amino acid serine in aqueous solution has also been studied by different authors. Tortonda et al.[60] use a B3PW91/6-31++G** level and the SCRF method to describe the solute−solvent interactions, obtaining very low energies, below those of alanine ($\Delta E^{\#}$ = 1.40 and ΔE_R = −2.95 kcal·mol^{-1}). Jeon et al.,[61] using the same level but the IEFPCM method, obtain a barrier higher than the corresponding of alanine, specifically $\Delta G^{\#}$ = 3.67 and ΔG_R = −5.17 kcal·mol^{-1}, and activation barriers even higher when an assisted mechanism is considered with two water molecules.[62]

There have been few theoretical studies of the neutral/zwitterionic tautomerization process for aspartic acid in aqueous solution.[63,64] Nagy et al,[63] using the PCM/RHF/631+G* model, report an unfavorable process in the gas phase (ΔE_R = 20.67 kcal·mol^{-1}) which is stabilized by the inclusion of various water molecules (obtaining a value of ΔE_R = −5.12 kcal·mol^{-1} when two water molecules are considered).

The context of these different, and sometimes contradictory, structural and thermodynamics results of the taumerización process in solution of these four amino acids lend the present study a certain importance for the purpose of comparison with the previous findings. Furthermore, we examine how the tautomerization process depends on the different chemical natures of the −R radical involved—hydrophobic in alanine, hydrophilic in serine and aspartic acid, and neutral as glycine.

With regard to the tautomerization mechanism, it is well know that the tautomeric equilibrium between neutral and zwitterionic forms of an amino acid is of importance in biochemistry and is extremely sensitive to the medium where the reaction occurs, which can be explained as reflecting the stronger interaction between the amino acids and the surrounding medium when the zwitterionic structure is present. Thus, in the gas phase these amino acids are usually in their neutral structure state, while in aqueous solution the zwitterionic form is the most stable.

The tautomerization reaction takes place as result of proton transfer between the neutral and zwitterionic forms. This requires an adequate orientation of the amino and acid groups involved in the transfer, and the presence of some water molecules leading to a more stable transition structure. Among the different mechanisms considered, we shall focus initially on internal proton transfer in water via a concerted and

nonassisted mechanism. Schematically this reaction is illustrated in Figure 1.

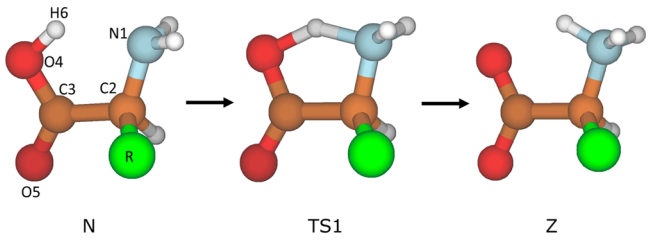

Figure 1. Nonassisted concerted mechanism.

In this mechanism, the hydroxyl hydrogen in the neutral structure (N) is transferred to the amino nitrogen, through a 5-member ring transition state (TS1) before moving to the zwitterionic structure (Z).

We also study the assisted concerted mechanism in water considering only one water molecule in the transition state, according to the scheme of Figure 2.

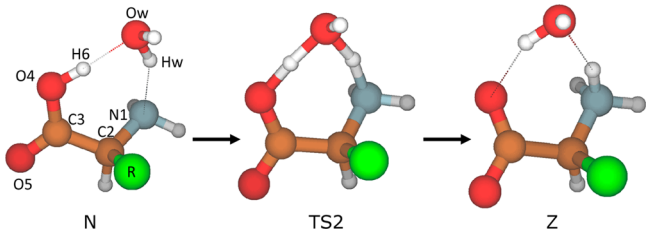

Figure 2. Assisted concerted mechanism.

In this case, the hydroxyl hydrogen in the neutral structure (N) is transferred to the water oxygen, and one of the water hydrogen atoms is simultaneously transferred to the amino nitrogen, forming a more stable ring of seven members (TS2) before moving to the zwitterionic structure (Z).

3. FORMALISM AND CALCULATION DETAILS

To describe solute−solvent interaction potential we use a LJ (12−6−1) function

$$U_{sw} = \sum_{ij} \frac{A_{ij}^{sw}}{r_{ij}^{12}} - \sum_{ij} \frac{B_{ij}^{sw}}{r_{ij}^{6}} + \sum_{ij} \frac{q_i^s q_j^w}{r_{ij}} \quad (1)$$

where the A_{ij}, B_{ij} van der Waals parameters are taken from the AMBER force field[23] for each type of atoms, instead of those from quantum calculations because of the great computational effort, and bearing in mind the smallness of the contribution of the van der Waals component to the whole interaction energy. However, the net charges on each solute atom q_i^s are obtained using the ASEP/MD procedure[41] from QM/MM calculations given the importance of the electrostatic component in this type of systems. The choice of these new parameters instead of those from our ESIE traditional procedure[30] is based on there being a simplification when molecules have a significant size, and moreover the ESIE charges are very similar to the proposed ASEP charges as will be seen in Results section for glycine in its neutral structure. Finally, the charges of the solvent water atoms q_j^w are preassigned as the TIP3P charges.[28]

To construct the free energy curves, we use as reaction coordinate the difference in the solute−solvent interaction energy of a given set of solvent molecules fluctuating in the presence of the reactant and product with their rigid structures,[65] for which one only needs the potential function that suitably describes the interaction. This technique has been widely employed to study electron transfer processes, and it has also been applied in proton transfer reactions.[66−68] Our procedure expands this method by including the information on the solvent in equilibrium with transition state in its optimal geometry, as well as those from the simulations of the solvation of the reaction and product (the zwitterion this case). The free energy curves are then calculated from comparison of these three situations taking in pairs. Thus, one can use the differences in the solute−water interaction energies (U_{sw}) between the diabatic states of the amino acid in two different structures for a broad set of configurations N_r of solvent molecules at each time step t_i from the simulation, with amino acid in its S configuration. For example, one can obtain the differences between the neutral (N) and zwitterionic (Z) structures with the solvent configurations of the S amino acid simulation (S could be either N or Z simulations):

$$\Delta E_S(t_i) = U_{sw,N}(t_{i,S}) - U_{sw,Z}(t_{i,S}) \quad (2)$$

One operates in a similar way to simulate the solvation of the transition state TS and its comparison with the N or Z states. The inclusion of the transition state step to obtain the activation free energies makes our method closer to the thermodynamic integration using the FEP method for the reactions considered in this work. The difference between them is that our procedure obtains the activation free energy in one step; meanwhile the thermodynamic integration requires several points and therefore several simulations; however our method is limited to the study of reactions with low energy barriers and without great changes in the geometry of the molecules involved in the reaction.

The values of ΔE_S fluctuate during the MD simulation, and their values are collected as a histogram of the number of times that a particular value Δe of the macroscopic variable ΔE_S appears in the simulation. The probability $P_S(\Delta e)$ of finding the system in a given configuration can be expressed[69]

$$P_S(\Delta e) = \frac{\sum_{i=1}^{N_r} \delta(\Delta E_S(t_i) - \Delta e)}{N_r} \quad (3)$$

where $\Delta E_S(t_i)$ is the value of the energy gap at the ith time step of the trajectory S. The delta function δ is assigned a value of 1 when $[\Delta E_S(t_i) - \Delta e] \leq (\Delta e_{max} - \Delta e_{min})/2n_{bins}$ and a value of 0 otherwise, where Δe_{max} and Δe_{min} are the maximum and minimum values of Δe that occurs during the trajectory and n_{bins} is the number of bins used to construct the histogram.[69,70,33,35]

This allows us to compute the free energy $G^S(\Delta e)$:

$$G^S(\Delta e) = -k_B T \ln P_S(\Delta e) \quad (4)$$

.

Next, a search is made for the polynomial function that best fits these free energies, and the results are plotted. To obtain a value of the $\Delta G^{\#}$ activation energies, the curve G^N is shifted at the intersection with the point of minimum energy of the curve G^{TS} (see ref 35 for a detailed description), where the separation between the two minima is given by

dx.doi.org/10.1021/jp307391s | J. Phys. Chem. B 2012, 116, 13033−13044

$$\Delta G^{\#} = G_{eq}^{N} - G_{eq}^{TS} = a(\Delta e_{eq}^{TS} - \Delta e_{eq}^{N}) + b(\Delta e_{eq}^{TS} - \Delta e_{eq}^{N})^2 + c(\Delta e_{eq}^{TS} - \Delta e_{eq}^{N})^3 + \ldots \quad (5)$$

with Δe_{eq}^{N} and Δe_{eq}^{TS} being the most probable values of Δe in the free energy curves G^N and G^{TS} respectively, and *a*, *b*, and *c*, are the coefficients of the polynomial fit to the curve G^N. The procedure is similar for the activation energies of the process Z → TS with the exception of the curve G^Z is now shifted.

When calculating the energy differences ΔE_S between the two states to construct the ΔG^S free-energy curves, it must be taken into account that it is necessary during the simulation of one of the molecules in water to place the other molecule in the position occupied by the first and reorient it in order to reproduce the position of their atoms. This is straightforward in the case of the nonassisted mechanism, but for the assisted mechanism the problem lies in how to position the two reactants (the separated neutral amino acid and one water molecule) or the two products (the separated zwitterionic amino acid and the water molecule) in order to carry out the simulation, since the solute−solvent interaction energies will depend notably on the separation and orientation of the two molecules. The correct way to do would be to situate them far apart so that there is no interaction between the two, but then the problem would arise that one would need very large simulation boxes to include both molecules. This would greatly increase the number of solvent molecules present, and hence the number of interactions. To solve this situation, we decided to change the strategy in constructing the free-energy curves, the neutral amino acid−water complex and the zwitterionic amino acid−water complex were employed in their optimal geometries as reactant and product, respectively, to make the superposition with the transition state structure (TS2). Then the stable contribution of the formation of each complex from their separated molecules was added to the activation and reaction energies.

Finally, some simulation details merit noting. We performed molecular dynamics simulations of an NVT ensemble of an amino acid molecule in an aqueous environment formed by about 210 water molecules were carried out at 298 K using the AMBER program.[71] The time considered for the simulations was 2000 ps with time steps of 0.1 fs. The first 1000 ps were taken to ensure that the equilibrium is reached completely; this was confirmed by the standard deviation of the potential energy values in the simulation being less than 1% of the mean value in all the cases. The last 1000 ps were stored, every 10 fs, to configurations of the water molecules required for the determination of the thermodynamic properties studied in this work. The water molecules initially located at distances less than 1.6 Å from any solute atom were eliminated from the simulations.

The long-range electrostatic interactions were treated by the Ewald method,[72] and the solutes were kept rigid using the shake algorithm.[73] A cutoff of 5 Å was applied to the water−water interactions to simplify the calculations, and periodic boundary conditions were used to maintain the number of solvent molecules constant.

4. RESULTS AND DISCUSSION

The presentation of the results is organized as follows. First, we shall show the optimal geometries in solution of reactants, products, and transition states for the different amino acids considered. We shall then present the ASEP atomic charges to define the solute−solvent interaction for each case. Then we shall analyze the contour maps of the solute−solvent interaction energy that drive the simulations, and we shall end with the thermodynamic results of the tautomerization reaction in its two versions—the assisted concerted and nonassisted concerted mechanisms—comparing them with those obtained in theoretical and experimental studies.

4.1. Geometries. Figure 3 shows the configuration obtained for the neutral form of each amino acid in the nonassisted and assisted mechanisms, obtained in solution at the 6-31G+**/MP2 level with the PCM model and the GAUSSIAN-09 program.[74] The hydroxyl group is oriented toward the amino group, facilitating the proton transfer of H6 hydrogen to N1 atom (nonassisted mechanism) or Ow atom (assisted mechanism) in the formation of intramolecular hydrogen bonds. This is consistent with results reported by other workers for amino acids in solution.[49,52,60,63]

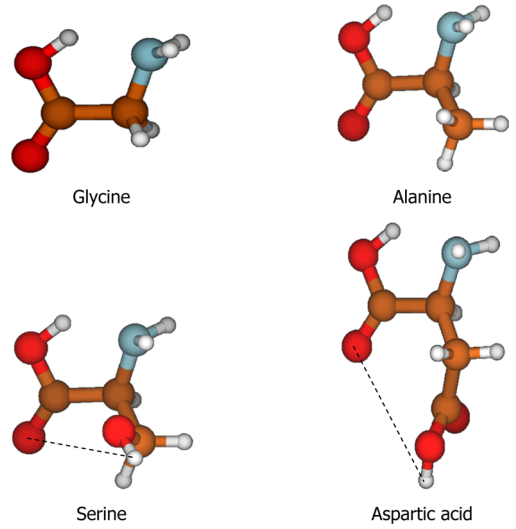

Figure 3. Representation of the -R group in the reactant structures.

For the serine and aspartic acid molecules, the hydroxyl and carboxyl groups respectively are oriented outward the molecule (see the orientation of the atoms of the −R group in Figure 3), away from other atoms that can establish intramolecular hydrogen bonds and avoiding a possible hydrogen transfer from the hydroxyl group (d_{H-O5} = 4.08 Å for serine case, marked with a dashed line) or carboxyl group (d_{H-O5} = 4.89 Å for aspartic case, also marked with a dashed line) to O5 oxygen.

Table 1 lists the geometric parameters described for the neutral, zwitterionic and transition state of the structures present in nonassisted mechanism (the TS2 structure of glycine in the assisted mechanism is also considered in this Table). All these optimized structures were calculated in the same conditions we have mentioned above for the neutral structure. They agreed with the results presented by other studies mentioned in section 2 above. One observes that the distances and bond angles hardly vary on going from one amino acid to another when the N, TS, and Z structures are compared, except logically the C2-R distance for the glycine case. We can say that the effect of the substituent is noticeable only in the dihedral angles depending on the type of substituent R considered.

dx.doi.org/10.1021/jp307391s | J. Phys. Chem. B 2012, 116, 13033−13044

Table 1. Geometric Parameters for the Different Structures of the Amino Acids

	glycine				alanine			serine			aspartic acid		
	N	TS1	TS2	Z	N	TS1	Z	N	TS1	Z	N	TS1	Z
C2−N1[a]	1.46	1.48	1..48	1.50	1.47	1.48	1.50	1.47	1.48	1.50	1.46	1.48	1.50
C2−C3	1.52	1.54	1.53	1.55	1.53	1.55	1.55	1.54	1.55	1.56	1.53	1.55	1.55
C3−O5	1.23	1.24	1.24	1.26	1.23	1.24	1.26	1.23	1.24	1.26	1.22	1.24	1.26
C3−O4	1.34	1.31	1.31	1.27	1.34	1.31	1.27	1.34	1.31	1.27	1.34	1.31	1.27
C2−R	1.09	1.09	1.09	1.52	1.52	1.52	1.53	1.52	1.51	1.51	1.53	1.52	1.52
O4−H6	1.00	1.21	1.13	–	1.00	1.21	–	1.00	1.23	–	0.99	1.24	–
N1−H6	–	1.31	–	1.04	–	1.30	1.04	–	1.27	1.04	–	1.27	1.04
O4−N1	2.57	2.37	2.89	2.56	2.55	2.36	2.55	2.56	2.36	2.56	2.56	2.36	2.57
H6−Ow	–	–	1.28	–	–	–	–	–	–	–	–	–	–
Ow−Hw	–	–	1.23	–	–	–	–	–	–	–	–	–	–
Hw−N1	–	–	1.25	–	–	–	–	–	–	–	–	–	–
N1−C2−C3[b]	109.6	104.0	114.0	107.8	108.2	103.1	106.3	108.6	103.2	107.0	108.4	103.0	106.7
O5−C3−C2	123.9	122.5	118.2	115.5	123.8	122.2	115.6	123.5	121.5	115.5	123.5	121.1	115.3
O4−C3−C2	113.9	110.6	119.1	115.1	114.0	111.1	115.2	113.9	110.8	119.5	114.1	110.9	114.9
N1−H6−O4	127.7	140.8	–	123.2	129.2	140.9	120.0	128.5	141.0	118.6	125.3	140.8	118.1
O4−H6−Ow	–	–	170.3	–	–	–	–	–	–	–	–	–	–
H6−Ow−Hw	–	–	86.0	–	–	–	–	–	–	–	–	–	–
Ow−Hw−N1	–	–	162.3	–	–	–	–	–	–	–	–	–	–
N1−C2−C3−O4[b]	10.4	0.0	36.2	0.9	5.6	0.3	14.8	7.1	3.0	10.5	20.1	6.7	19.5
C3−C2−N1−H6	9.0	0.0	–	1.4	5.1	0.6	20.2	6.7	3.2	19.0	16.7	6.0	24.7
C3−C2−N1−Hw	–	–	52.9	–	–	–	–	–	–	–	–	–	–

[a]Distances in Å. [b]In degrees.

Table 2. Atomic Charges for the Different Amino Acids

	glycine						alanine			serine			aspartic acid		
	N														
atom	ASEP	ESIE	Mulliken	TS1	TS2	Z	N	TS1	Z	N	TS1	Z	N	TS1	Z
N1	−0.99	−0.99	−0.81	−0.65	−0.32	−0.42	−1.07	−0.83	−0.63	−1.01	−0.74	−0.50	−1.10	−0.89	−0.73
H	0.41	0.41	0.35	0.38	0.30	0.37	0.43	0.41	0.40	0.44	0.38	0.40	0.44	0.43	0.44
H	0.42	0.38	0.34	0.38	0.30	0.37	0.41	0.40	0.43	0.40	0.41	0.37	0.43	0.44	0.45
C2	0.24	0.06	−0.05	0.04	−0.05	0.01	0.43	0.32	0.30	0.25	0.11	0.15	0.46	0.40	0.40
H	0.01	0.08	0.19	0.08	0.07	0.10	0.01	0.03	0.02	0.02	0.05	0.04	0.01	0.02	0.02
R	0.04	0.14	0.20	0.08	0.09	0.09	−0.05	−0.01	0.02	0.01	0.04	0.03	−0.11	−0.10	−0.06
C3	0.98	0.92	0.61	1.05	1.05	1.07	0.91	0.97	1.01	1.00	1.05	1.06	0.88	0.90	0.95
O5	−0.87	−0.76	−0.70	−0.93	−0.89	−0.99	−0.84	−0.90	−0.97	−0.84	−0.92	−0.98	−0.79	−0.85	−0.94
O4	−0.64	−0.73	−0.60	−0.78	−0.84	−0.93	−0.67	−0.79	−0.94	−0.69	−0.82	−0.94	−0.67	−0.79	−0.95
H6	0.40	0.45	0.45	0.35	0.59	0.32	0.43	0.41	0.40	0.44	0.41	0.37	0.44	0.45	0.42
Ow[a]					−1.15										
Hw[a]					0.33										

[a]In an isolated molecule, the charges are: $\delta(O) = -0.83$ and $\delta(H) = 0.415$.

In relation to the TS1 transition state structures, one can say that, on its way from the neutral to the zwitterionic, O4−H6 distance increases about 0.2 Å. In all the cases, the process goes through a lengthening of O4−H6 bond to put the hydrogen at a distance of about 1 Å of the N1 nitrogen. Also, this transition structure is found to be a nearly planar ring of 5 members, with very similar distances and bond angles.

When a water molecule is included as taking part in the reaction mechanism (only in the glycine case), the TS2 transition state obtained shows that Hw hydrogen links to the amine nitrogen, and the H6 hydrogen links to the Ow oxygen of the water molecule. One also observes in Table 1 that the length of the Ow−Hw bond increases to 1.23 Å, with the Ow oxygen at 1.28 Å from the H6 hydrogen, and the O4−H6 distance increases slightly, which permits the liberation of the H6−Ow−Hw water molecule that is different from the original water molecule that assists in the mechanism. In the TS2 transition states, the formation of a nonplanar ring of seven members makes the structure less stressed than the TS1 structure with more open bond angles, especially the Ow−Hw−N1 and O4−H6−Ow angles with atoms involved in the proton transfer.

Considering the zwitterionic structures we can appreciate that the carbonyl double bond is now delocalized between the two oxygen atoms, and the two C−O distances become quite similar. Another important effect observed is that the N1−O4 distance decreases along the N → TS process and then returns nearly to the original distance in the TS → Z process. Finally, the bond and dihedral angles are the largest deviations from the values present in the neutral structures.

These TS1 and TS2 transition states were verified by carrying out a normal-mode analysis, which provides a single imaginary frequency ($\upsilon_{TS1} = -1198$ cm^{-1}; $\upsilon_{TS2} = -1258$ cm^{-1} for the glycine case) and whose eigenvector corresponds to the

dx.doi.org/10.1021/jp307391s | J. Phys. Chem. B 2012, 116, 13033−13044

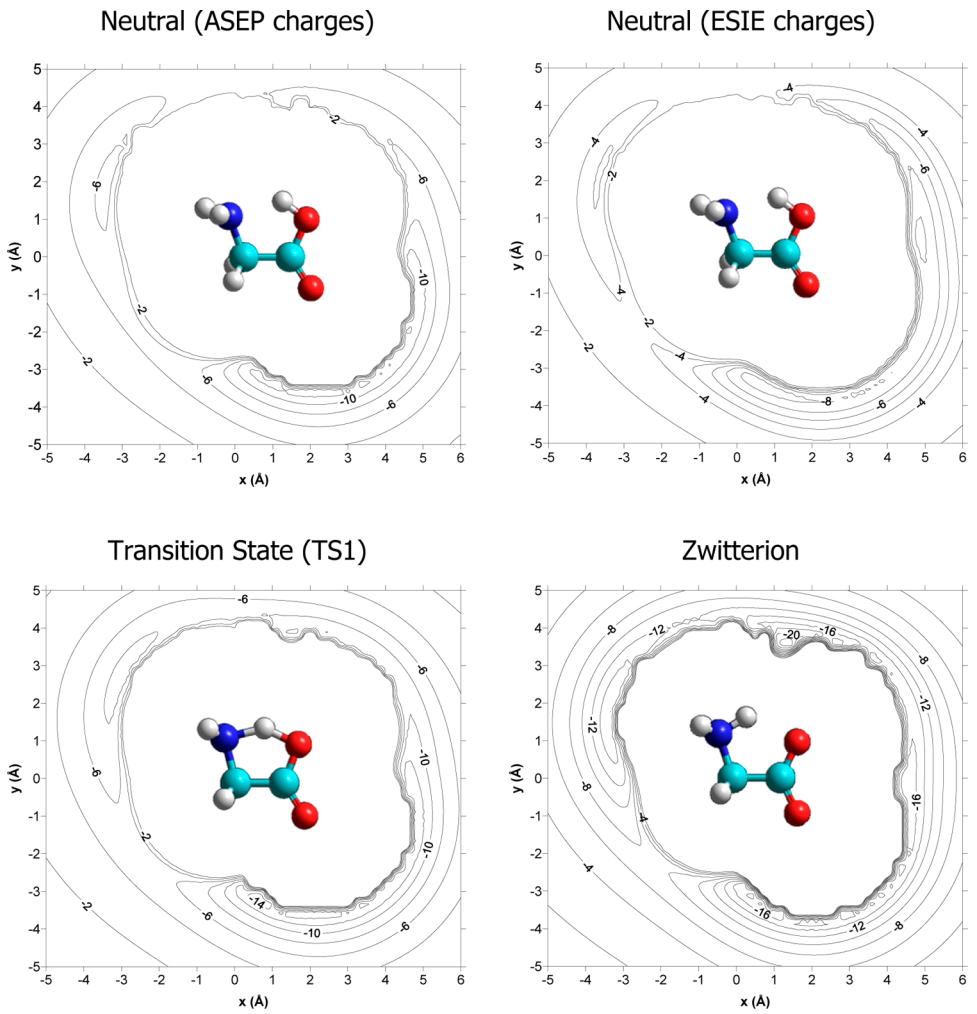

Figure 4. Contour maps for the N, TS, and Z glycine configurations at $z = 0$.

simultaneous breaking of the O4−H6 bond to form the N1−H6 bond in the TS1 case, and the rupture O4−H6 and Ow−Hw bonds to form the H6−Ow and N1−Hw bonds in the TS2 case. It is important to note that, with the above result, the mechanism of the reaction in solution can therefore be assumed to proceed through a single transition state (concerted mechanism), rather than stepwise mechanism.

4.2. ASEP Charges. Table 2 lists the ASEP atomic charges obtained for the different amino acids studied in this work with a QM/MM procedure. This method uses the ASEP/MD code[41] that employs a mean field approximation to represent the solute−solvent interaction and the MOLDY program[75] for the molecular dynamics calculation. ESIE and Mulliken charges for glycine in its neutral structure are also included for the sake of comparison. It can be seen that ASEP charges are greater than Mulliken ones obtained from MP2/PCM calculations, but they are in better agreement with ESIE charges obtained with our procedure as we mentioned above.

There is no important variation in these charges for the neutral structure as one goes from one amino acid to another. The greatest of these variations occurs on the C2 atom bond to −R group, as a result of the different nature of this group for each amino acid. While the −R group in glycine and serine presents the same positive charge, negative charge on this group (−0.05e in alanine and −0.11e in aspartic acid) produce a more positive charge on C2 atom. These variations affect the charge on atoms neighboring the C2 atom, especially on the N1 nitrogen.

In the formation of the transition state TS1, the charge on the N1 nitrogen decreases and the charge on the O4 atom increases. I.e., there is a flow of electronic charge from the N1 to O4 during the tautomerization process.

For the case of considering the TS2 transition state with a water molecule in the ring, one observes an increase of the charge on the Ow atom, which produces an increase of positive charge on H6 greater than that produced in TS1 transition. Similarly, there is a decrease of the negative charge on the N1 atom, which is more pronounced than in TS1 case, meaning that the flow of charge from O4 to N1 atom is also greater.

Comparison of the charges between the neutral and zwitterionic structures give results that are similar to those mentioned above; i.e., there is a decrease in charge on the N1 atom and an increase on the O4 atom, although these variations are now more pronounced, with the resulting structures being more charged. Also, the charges on the O4 and O5 oxygen atoms, which are different in neutral structures, are similar in zwitterionic structures, thus explaining the existing molecular resonance.

4.3. Contour Maps. An analysis of the LJ interaction function U_{sw} has also been carried out to compare the different potentials for the amino acids considering that the small differences in geometry parameters and charges between the

dx.doi.org/10.1021/jp307391s | J. Phys. Chem. B 2012, 116, 13033−13044

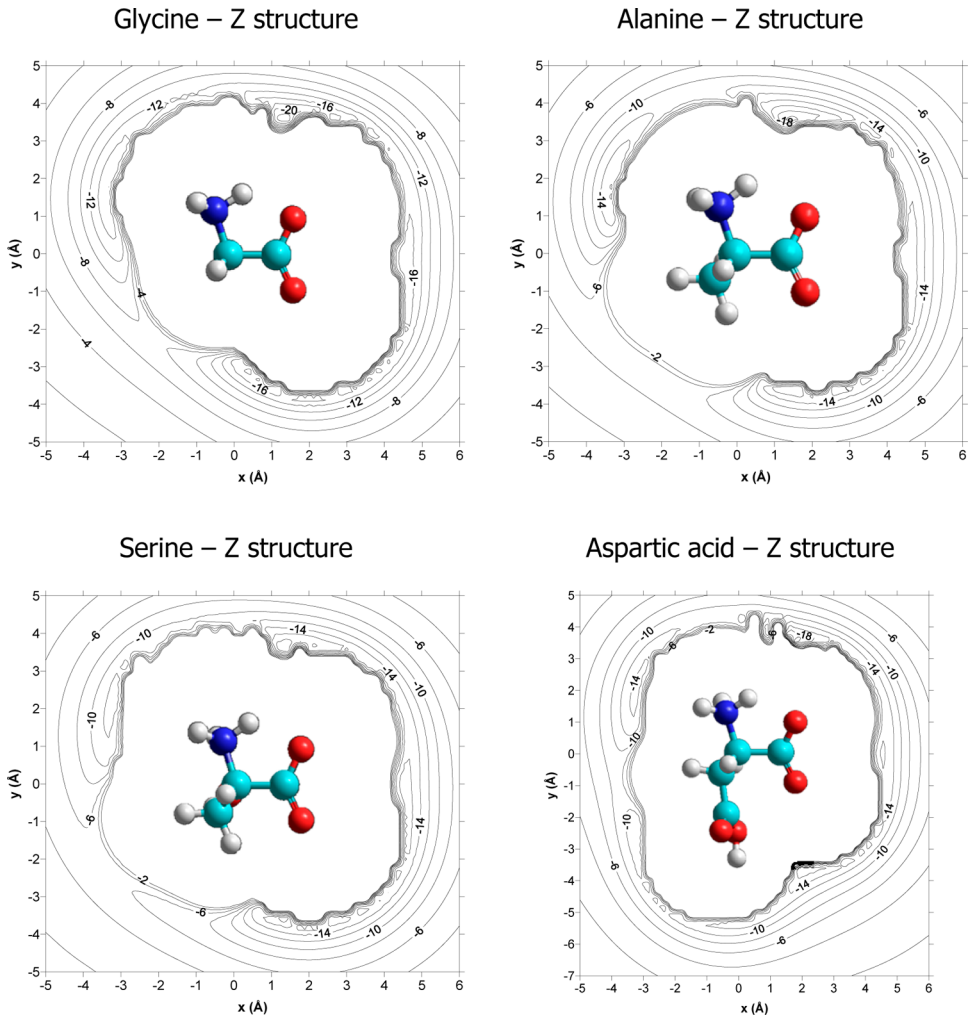

Figure 5. Contour maps for the Z configurations at $z = 0$ of the amino acids considered.

four amino acids at each structure were hardly sufficient to clarify the different behavior of those amino acids in the tautomerization process. Potential contour maps for all the amino acids in the N, TS, and Z structures of the reaction were calculated for a three-dimensional grid of points around the amino acid. To this end, a water molecule was located with its center of mass successively at each point of the grid, and it was oriented to provide the minimum interaction energy. In order to be able to compare the maps, the amino acids were situated in the same configuration, the plane formed by the N1−C2−C3 atoms have situated on the *xy* plane, at $z = 0$, the C2 atom was at the coordinate center, the bond C2−C3 is along the positive *x* axis and the angle N1−C2−C3 is taken counterclockwise. Several contour maps were constructed at different values of the *z* coordinate.

The contour maps at $z = 0$ for glycine in its N, TS1, and Z configurations are shown in Figure 4. This also included the contour map obtained from ESIE procedure for the N structure to show the similarity between both methods that was mentioned above. It can be seen that there exist some common features. First, there is a deep minimum (12−16 kcal·mol^{-1}) around the O5 atom in all the cases. This is due to the high charge on this atom and because its external position allows hydration without any interferences. The second similarity is the minimum (6−14 kcal·mol^{-1}) around the $-NH_2$ group. Again, this is the result of the hydration of the two hydrogen atoms of that group. Both of these minima become deeper during the tautomerization process because of the change in the charge of these atoms. Thus, the O5 atomic charge increases from the N to the Z configuration for all the amino acids, and consequently the minimum around this atom changes from −12 to −16 kcal·mol^{-1}. For the minimum close to $-NH_2$ group, although the hydrogen atomic charges barely change, the N1 charge decreases in value significantly during tautomerization, but the presence of H6 atom in this zone in the Z structure favors the hydration of this $-NH_3$ group (the minimum depth changes from −6 to −12 kcal·mol^{-1}). One has to bear in mind that the AMBER parameters are equal for the configurations of the same amino acid except for O4 and H6 atoms which change their type.

The same conclusions can be drawn for these two minima when considering the rest of the amino acids. Obviously, there exist other minima close to the different radicals R of each amino acid, but they do not change along the tautomerization process and their influence is constant.

The main change in the interaction energy during tautomerization appears in the region of the O4−H6−N1 bridge. From a poorly localized minimum of about −2 or −4 kcal·mol^{-1} in the neutral configuration, a deeper, strongly localized minimum of −22 kcal·mol^{-1} appears near the bridge in the zwitterionic form. This minimum extends below and behind the amino acid O4−H6−N1 plane. In particular, it

dx.doi.org/10.1021/jp307391s | J. Phys. Chem. B 2012, 116, 13033−13044

spans near 2 Å toward both sides. The stability of the zwitterionic structures is due to this interaction.

Comparing the interaction around the bridge for the amino acids studied, we found the same shallow minimum in the neutral structure that becomes deeper in the zwitterionic structure in all the cases. But there exists an important difference in alanine and especially in serine. In both cases, the minimum behind the bridge plane (negative values of z) becomes shallow due to the presence of the R radical. Moreover, in the serine case, the depth of the minimum is about 4 kcal·mol^{-1} less than for the rest of the amino acids because of the position of the oxygen atom of the alcohol group that is near the amine group, as we can see in Figure 3. To picture of the hydration process of the zwitterionic structure, one must imagine the water molecules heading their Hw hydrogen atoms toward the O4 atom and the Ow oxygen to the H6 atom bonded with the amine group. In this configuration the oxygen atom of the alcohol group in the radical of serine interferes negatively with the hydration.

Contour maps of the four amino acids in their zwitterionic structures at $z = 0$ are shown in Figure 5. One sees see that the minima around the bridge in alanine and serine are shallower than in the glycine and aspartic acid cases, as we mentioned above. Therefore, lower solvation energies may be expected for alanine and serine.

4.4. Thermodynamic Properties. Figure 6 shows the activation and reaction energies of glycine for assisted and nonassisted mechanism. These energies are evaluated using the G^N, G^{TS1}, G^{TS2}, and G^Z diabatic free energy curves obtained from U_{sw} energies using the procedure describe in the formalism section (section 3). For the activation energies, the G^N and G^{TS} curves are employed for the N → TS process and, consequently the G^Z and G^{TS} curves for the Z → TS process.

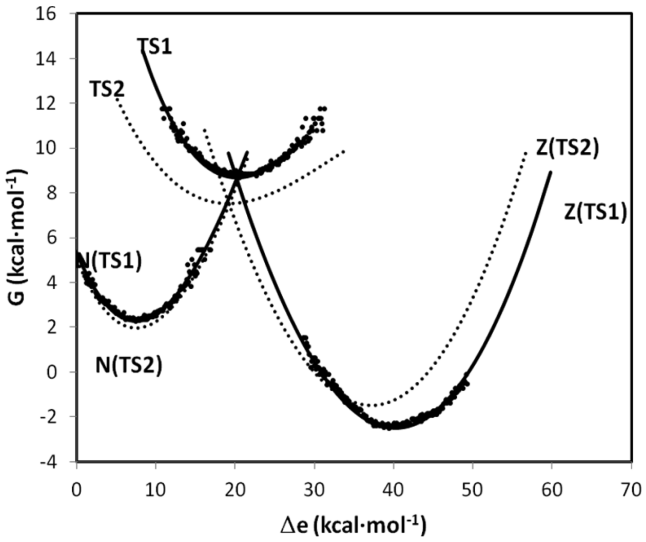

Figure 6. Free energy curves for R, TS and Z states of glycine (solid line for N → TS1 → Z process and dotted line for N → TS2 → Z process).

The relative positions of these curves were modified in accordance with our previous studies, where the curves were shifted vertically to the point of intersection $G^N(\Delta e) = G^{TS}(\Delta e_{eq})$ for the direct activation energies and $G^Z(\Delta e) = G^{TS}(\Delta e_{eq})$ for the inverse activation energies. The difference between the direct and inverse activation energies gives the reaction energy.

When one allows the mechanism to be assisted by one solvent water molecule, the $G^{N,[TS2]}$ energy curve is similar to the nonassisted one $G^{N,[TS1]}$ but the $G^{TS,[TS2]}$ curve is deeper leading to a slight decrease of the energy barrier. Similarly, the curve for the product $G^{Z,[TS2]}$ turns out to be shallower than $G^{Z,[TS1]}$, so that a lower reaction energy is obtained.

The results presented in Table 3 show the dependence of the free energies of reaction ΔG_R and activation $\Delta G^{\#}$ for the glycine with the different states and level of calculation considered in this work. In the gas phase for both the assisted and nonassisted mechanisms, the tautomerization process N → Z is clearly unfavorable, with higher activation barriers and very endothermic reaction energies (reduced when the calculations are carried out at the MP2 level). In aqueous solution, either by the PCM or the MD/MP2 method, there is a significant reduction of the activation barrier, leading to small reaction energies of the process being obtained (they even are exothermic for both mechanisms with the MD/MP2 procedure). In order to determine the error of our MD/MP2 results, several simulations were carried out using different equilibrium times and therefore different simulation starting point, obtaining an associated error of ±5% in the free energy values presented.

The values of the activation and reaction free energy obtained for the tautomerization of glycine with the nonassisted mechanism and the MD/MP2 method are good when compared with the experimental results,[42−45] improving those obtained by us with the PCM/MP2 method and by other authors,[48−50] and in good agreement with the values of Nagaoka,[46] Rahaman[51] and Cui.[55] A thermodynamic integration using the FEP method has been carried out, obtaining a value of $\Delta G^{\#}$ = 6.43 kcal·mol^{-1} for glycine which can be expected as it was mentioned in section 3 and validates the result of our method.

An additional comment would be in order for the MD/MP2 values given in the Table 3 and illustrated in reaction path of Figure 7 for the two concerted mechanisms. That the MD/MP2 results are similar for the two mechanisms may appear to indicate that the assisted mechanism (shown by solid lines in the figure) also favors the tautomerization process. One must bear in mind, however, that the correction due to the additional stabilization produced when the separate reactants (Gly(N) and Water) form the complex (Gly(N)−water) leads to lower energies of smaller activation ($\Delta G^{\#}$ = 0.84 kcal·mol^{-1}) and reaction energies (ΔG_R = −1.31 kcal·mol^{-1}) than in the nonassisted mechanism (dot-dashed and dotted lines, respectively). With this correction, the nonassisted mechanism prevails over the assisted mechanism with one water molecule in the glycine tautomerization, as is consistent with available experimental and theoretical results. Given that this additional stabilization of the amino acid−water complex will be similar in all the cases, it is reasonable to extend the same conclusion to the rest of amino acids, although further calculations should be carried out to check the validity of this supposition depending on the election of the factors that affect the numerical results (basis set, level of calculation, simulation parameters, ...). We shall continue by addressing the thermodynamic study of other amino acids only with the nonassisted mechanism.

The charges and geometries presented in Tables 1 and 2 for the different amino acids affect the U_{sw} interaction energies calculated by eq 1, which are given for the nonassisted

Table 3. Activation and Reaction Free Energies[a] for the Glycine

			$\Delta G^{\#}$	ΔG_R
nonassisted	gas	SCF	20.11	25.81
		MP2	11.56	20.65
	solution	PCM/SCF	12.21	3.89
		PCM/MP2	4.53	0.73
		MD/MP2	6.64	−4.91
assisted	gas	SCF	24.75 (22.03)[b]	16.15 (29.65)
		MP2	13.40 (6.77)	13.23 (26.04)
	solution	PCM/SCF	16.07 (15.51)	−4.60 (−1.78)
		PCM/MP2	5.51 (1.16)	−5.97 (−3.01)
		MD/MP2	5.29 (0.84)	−4.27 (−1.31)
experimental			6.90	−7.30

[a]In kcal·mol^{-1}. [b]The values in between parentheses correspond to using the energy of the amino acid separated a distance of 20 Å from the water molecule.

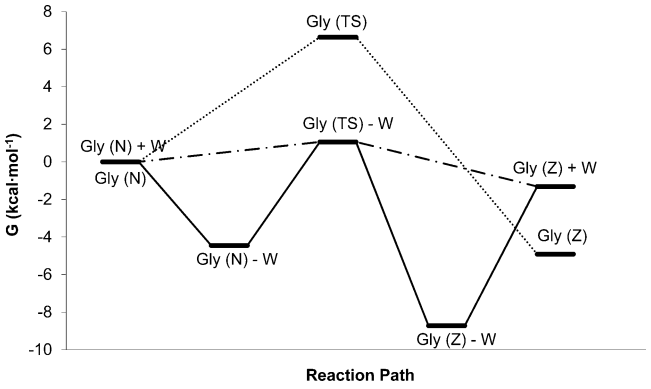

Figure 7. Free energy profile for glycine using an assisted mechanism and a MD/MP2 calculation.

mechanism at MD/MP2 level in Table 4. In this table, each average value $<U_X - U_Y>_S$ represents the difference in an amino acid's solute−solvent interaction energy when its structure changes from X to Y during the simulation performed using the solute structure S; i.e. the average value of the difference in its interaction energy within the water environment when the amino acid switches to a different structure. This is equivalent to the comparison of the Δe values for the G^X and G^Y minima presented in Figure 6. Thus, $\Delta U^{\#}$ in this table is related with the separation Δe in Figure 6 between the points associated with the activation barrier for the N → TS process, and ΔU_R the separation Δe between the points associated with the reaction energy for the N → Z process.

Table 4. Variation of the Interaction Energies[a] with the Solute Structure

	$\langle U_N - U_{TS}\rangle_N$	$\langle U_N - U_{TS}\rangle_{TS}$	$\langle U_{TS} - U_Z\rangle_Z$	$\Delta U^{\#}$ [b]	ΔU_R [c]
glycine	7.8	20.9	38.5	13.1	30.7
alanine	9.2	18.4	39.7	9.2	30.5
serine	10.5	19.0	32.4	8.5	21.9
aspartic acid	9.6	23.7	49.0	14.1	39.4

[a]In kcal·mol^{-1}. [b]$\Delta U^{\#} = \langle U_N - U_{TS}\rangle_{TS} - \langle U_N - U_{TS}\rangle_N$. [c]$\Delta U_R = \langle U_{TS} - U_Z\rangle_Z - \langle U_N - U_{TS}\rangle_N$.

With respect to the results presented in this table, one observes that the greatest energy differences with the switch of structures occur when a zwitterionic structure is present. Given the relationship between the separations Δe and the activation and reaction energies (the highest energy should correspond to the greatest separation), one can predict that the tautomerization process with highest activation barrier and reaction energies will be that of aspartic acid, and the lowest that of serine.

Table 5 and Figure 8 present the free energy results for the four amino acids considering only the nonassisted concerted mechanism (in Figure 8 all the G^N curves have been represented with a single curve given the similarity between them); one can appreciate how well they maintain the observations made for glycine. The aqueous medium reduces

Table 5. Activation and Reaction Free Energies[a] for Amino Acids

	$\Delta G^{\#}$			ΔG_R		
	GAS	*PCM*	*MD*	*GAS*	*PCM*	*MD*
glycine	11.56	4.53	6.64	20.65	0.73	−4.91
alanine	10.88	4.13	4.87	19.80	0.65	−2.14
serine	10.88	4.30	4.38	18.82	0.20	−2.04
aspartic acid	12.46	5.15	6.78	21.06	1.34	−5.81

[a]In kcal·mol^{-1}; at MP2 level.

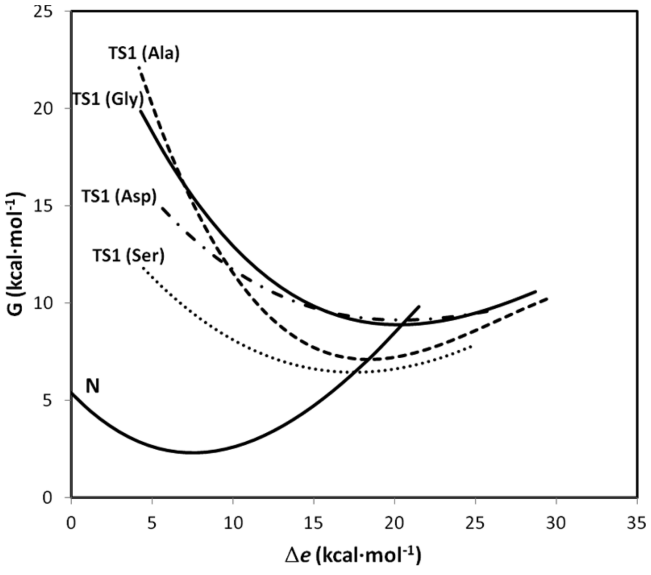

Figure 8. Free energy curves for N and TS1 states of the amino acids considered.

dx.doi.org/10.1021/jp307391s | J. Phys. Chem. B 2012, 116, 13033−13044

the activation barrier between 5 and 7 kcal·mol^{-1} and the reaction energy between 21 and 26 kcal·mol^{-1} in comparison with the gas phase. The solvent has to be described as discrete to obtain exothermic processes in better agreement with the available data. The values given in Table 5 are in agreement with the results presented in section 2, especially with those for which the description of the solvent considered was discrete.

The values obtained for the activation barrier and the reaction energy of the alanine tautomerization reaction were lower than for glycine case, consistent with those of other workers.[57] This was to be expected given the greater solvation free energy of glycine respect to alanine. Likewise, the experimental values of the rate constants (k = 8.0 × 10^{-5} s^{-1} for glicine and 21.2 × 10^{-5} s^{-1} for alanine) and equilibrium constants (k_{eq} = 31 × 10^{-3} for glicine and 11 × 10^{-3} for alanine) in a basic OH$^-$ medium[76] also validate these results. To understand this, one must consider the variation of the electrostatic component of the solute−solvent interaction energies with the change of structure of these two amino acids (Table 4). Given the similarity in size of the two molecules, and consequently the similarity in their entropy component, one can understand that the smaller separation Δe (see also Figure 8) between the minima in alanine than in glycine leads to the former having the lower activation barrier and reaction energy.

A similar analysis holds for the other amino acids to understand their barrier and free reaction energies on the basis of the solute−solvent electrostatic interaction energies. In this context, one expects that serine has a lower activation barrier and reaction energy than alanine and glycine, and that the aspartic acid must have the highest energies of the four. The different behavior of serine and aspartic acid may seem surprising given their hydrophilic character, but it has to be taken into account that the solvation energy of the serine is similar to that of alanine, but is the greatest of all for aspartic acid, as can be seen in the contour maps of Figure 5.

In this sense, it is important to recall the differences of the U_{sw} interaction energy seen in the contour maps. The presence of the −R group in alanine and especially in serine makes the solvation of the zwitterionic structures of these two amino acids less stable. As was mentioned above, all four amino acids behave similarly in the N structure, but differ importantly in the zwitterionic structure. This can be seen from the radial distribution function $g(r)$ of the solvent atoms with respect to the solute. Figure 9 shows $g(r)$ between the H6 atom and the Ow solvent atom for all four amino acids in their N configuration, and Figure 10 shows $g(r)$ between the O4 solute atom and the Hw atom for the Z configuration.

In the neutral case, the radial distribution functions show a poorly defined structure of the solvent molecules around the H6 atom, concordant with the pooly localized minimum close to the bridge O4−H6−N1. Therefore, there should be no differences between the four amino acids obtained from their hydration in the N structure. However, considering the $g(r)$ of the Z structures, one observes a well-defined solvent structure. A first coordination sphere appears at the same distance (around 1.6−1.7 Å) in all the cases, but their heights are quite different, the lowest being those for serine and alanine. The coordination number also reflects the better hydration of glycine (n_c = 1.8) and aspartic acid (n_c = 1.5) than of alanine (n_c = 0.5) and serine (n_c = 1.1). The low level of hydration of alanine in this first coordination sphere might lead one to think that the reaction energy for alanine would be the lowest, but

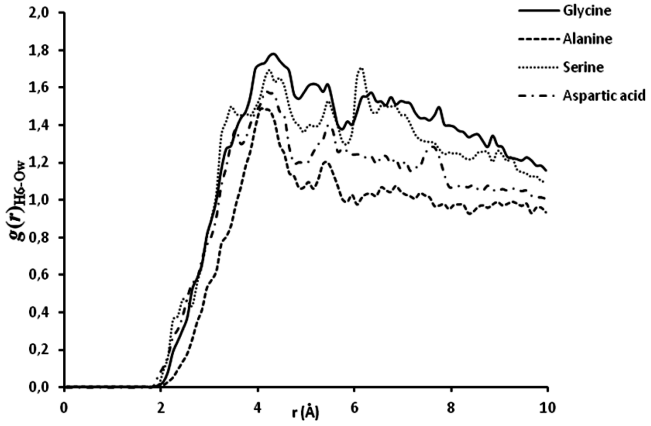

Figure 9. Radial distribution function $g(r)_{\text{H6-Ow}}$ of the amino acids considered in their N configuration.

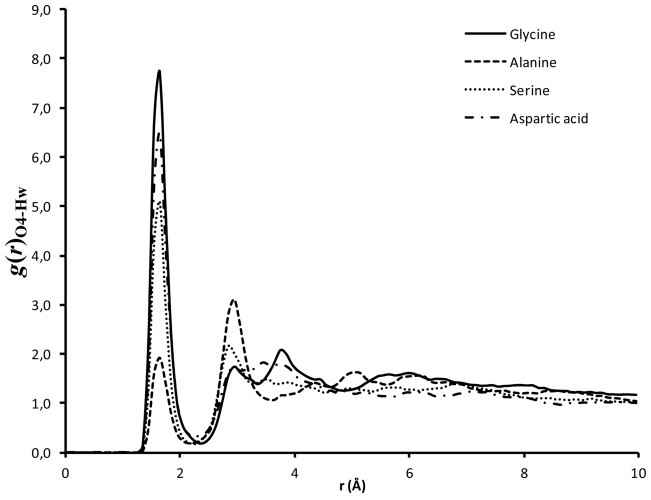

Figure 10. Radial distribution function $g(r)_{\text{O4-Hw}}$ of the amino acids considered in their Z configuration.

when the second sphere is considered the hydration of alanine (n_c = 5.0) is better than in serine (n_c = 3.6) case. A similar situation is observed for glycine and aspartic acid curves.

5. CONCLUDING REMARKS

In this work we have examined the tautomerization reaction of four amino acids using free energy curves obtained from MD simulation. The solvent have been used as the reaction coordinate and the role of the solvent in the mechanism have been studied.

Concerning the charges over the solute atoms, it can be observed that the values obtained using our ESIE procedure are quite similar to those from the ASEP methodology (QM/MM) and both drives to analogous results.

The normal-mode analysis of the transition states of the two concerted mechanisms (assisted and nonassisted) illustrates that the reaction in solution goes on through a single transition state (concerted mechanism), rather than stepwise mechanism.

The free-energy curves of the reactant, transition state, and products, obtained by MD simulations from optimized geometries in solution and with QM/MM charges have shown themselves to be very useful for the study of chemical reactions in solution. These curves provide an acceptable response to the reaction and activation energies of the

tautomerization thermodynamics of amino acids in an aqueous medium. And finally, we consider that, to obtain results matching the available experimental and theoretical data, one has to describe the solvent as a discrete medium and consider the nonassisted concerted mechanism.

AUTHOR INFORMATION

Corresponding Author

*Telephone: +34-924289300. Fax: +34-924275576. E-mail: santi@unex.es.

Notes

The authors declare no competing financial interest.

ACKNOWLEDGMENTS

This research was sponsored by the Consejería de Infraestructuras y Desarrollo Tecnológico de la Junta de Extremadura (Project GRU10036).

REFERENCES

(1) Cramer, C. J.; Truhlar, D. G., Eds. *Structure and Reactivity in Aqueous Solution: Characterization of Chemical and Biological Systems*, American Chemical Society: Washington D.C., 1994.

(2) Warshel, A. *Computer Modeling of Chemical Reactions in Enzymes and Solutions*; Wiley & Sons: New York, 1991.

(3) Jortner, J.; Levine, R. D.; Pullman, B., eds., *Reaction Dynamics in Cluster and Condensed Phases*; Kluwer Acad. Pub.: Dordrecht, The Netherlands, 1994.

(4) Moreau, M.; Turq, P. *Chemical Reactivity in Liquids*. Fundamental Aspects, Plenum Pub. Corp.: New York, 1988.

(5) Hoheisei, C. *Theoretical Treatment of Liquids and Liquid Mixtures*; Elsevier: Amsterdam, 1993.

(6) Politzer, P.; Murray, J. S., Eds. *Quantitative Treatments of Solute Solvent Interactions*; Elsevier: Amsterdam, 1994.

(7) Simkin, B. Y.; Sheikhet, I. I. *Quantum Chemical and Statistical Theory of Solutions. A Computational Approach*: Ellis Horwood: London, 1995.

(8) Truhlar, D. G.; Isaacson, A. D.; Garret, B. C. *The Theory of Chemical Reaction Dynamics*; Baer, M., Ed.; CRC Press: Boca Raton, FL, 1985; Vol. 4.

(9) Muller, A.; Ratjczak, H.; W. Junge, W. *Electron and Proton Transfer in Chemistry and Biology*; Diemann, E., Ed.; Elsevier: Amsterdam, 1992.

(10) Bala, P.; Grocowski, P.; Lesyg, B.; McCammon, J. A. *Quantum Mechanical Simulation Methods for Studying Biological Systems*; Bicout, D. M. F., Ed.; Springer: Berlin, 1995.

(11) Gao, J. Methods and Applications of Combined Quantum Mechanical and Molecular Mechanical Potentials. In *Review in Computational Chemistry*; Lipkowitz, K. B., Boyd, D. B., Eds.; Wiley-VCH: Weinheim, Germany, 1996; Vol. 7.

(12) Rivail, J. L. Solvent Effects on Potential Energy Surface and Chemical Kinetics. In *New Theoretical Concepts for Understanding Organic Reactions*; Bertrán, J., Csizmadia, I. G., Eds.; Kluwer Academic Publisher: Dordrecht, The Netherlands, 1989.

(13) Cramer, C. J.; Truhlar, D. G. Continuum Solvation Model, *In Solvent Effects and Chemical Reactivity*; Tapia, O., Bertrán, J., Eds.; Kluwer Academic Publisher: Dordrecht, The Netherlands, 1996.

(14) Hynes, J. T. Crossing the Transition State in Solution, *In Solvent Effects and Chemical Reactivity*; Tapia, O., Bertrán, J., Eds.; Kluwer Academic Publisher: Dordrecht, The Netherlands, 1996.

(15) Truhlar, D. G. *Direct Dynamics Method for the Calculation of reaction Rates, in the Reaction Path in Chemistry: Current Approaches and Perspectives*; Heidrich, D., Ed.; Kluwer Academic Publisher: Dordrecht, The Netherlands, 1995.

(16) Aqvist, J. Modelling of Proton Transfer Reactions in Enzymes. In *Computational Approaches to Biochemical Reactivity*, Naray-Szabó, G., Warshel., A., Eds.; Kluwer Academic Publisher: Dordrecht, The Netherlands, 1997.

(17) Binder, K.; Ciccotti, G.; Ferrario, M. Computer Simulations in Condensed Matter Systems. In *From Materials to Chemical Biology*; Springer: Berlin, 2006; Vol. 2.

(18) Levine, R. D. *Molecular Reaction Dynamics*; Cambridge Univ. Press: London, 2005.

(19) Miertus, S.; Scrocco, E.; Tomasi, J. *Chem. Phys.* **1981**, *55*, 117−129.

(20) Gao, J. *J. Phys. Chem.* **1992**, *96*, 537−540.

(21) Car, R.; Parrinello, M. *Phys. Rev. Lett.* **1985**, *55*, 2471−2474.

(22) Alder, B. J.; Wainwright, T. E. *J. Chem. Phys.* **1959**, *31*, 459−466.

(23) Cornell, W. D.; Cieplak, P.; Bayly, C. I.; Gould, I. R.; Merz, K. M.; Ferguson, D. M.; Spellmeyer, D. C.; Fox, T.; Caldwell, J. W.; Kollman, P. A. *J. Am. Chem. Soc.* **1995**, *117*, 5179−5197.

(24) Jorgensen, W. L.; Maxwell, D. S.; Tirado-Rives, J. *J. Am. Chem. Soc.* **1996**, *118*, 11225−11236.

(25) Brooks, B. R.; Bruccoleri, R. E.; Olafson, B. D.; States, D. J.; Swaminathan, S.; Karplus, M. *J. Comput. Chem.* **1983**, *4*, 187−217.

(26) Hermans, J.; Berendsen, H. J. C.; van Gunsteren, W. F.; Postma, J. P. M. *Biopolymers* **1984**, *23*, 1513−1518.

(27) Lii, J.-H.; Allinger, N. L. *J. Comput. Chem.* **1991**, *12*, 186−199.

(28) Jorgensen, W. L.; Tirado-Rives, J. *J. Am. Chem. Soc.* **1988**, *110*, 1657−1666.

(29) Tolosa, S.; Hidalgo, A.; Sansón, J. A. *Chem. Phys.* **2001**, *265*, 207−215.

(30) Tolosa, S.; Sansón, J. A.; Hidalgo, A. *Chem. Phys. Lett.* **2002**, *357*, 279−286.

(31) Tolosa, S.; Sansón, J. A.; Hidalgo, A. Simulation of Chemical Processes in solution using ab initio energies. In *Recent Research Developments in Chemical Physics*; Transworld Research Network: Kerala, India, 2002; Vol. 3.

(32) Tolosa, S.; Sansón, J. A.; Hidalgo, A. *Chem. Phys.* **2006**, *327*, 187−192.

(33) Tolosa, S.; Sansón, J. A.; Hidalgo, A. *J. Phys. Chem. A* **2007**, *111*, 339−344.

(34) Tolosa, S.; Sansón, J. A.; Hidalgo, A. Molecular Dynamics simulations of chemical processes in solution using potentials based on solute-solvent interaction energy components: Application to structural, dielectric, and energy properties. In *Quantum Chemistry Research Trends*; Kaisas, M. P., Ed.; Nova Science Publisher: New York, 2007.

(35) Tolosa, S.; Corchado Martín-Romo, J. C.; Hidalgo, A.; Sansón, J. A. *J. Phys. Chem. A* **2007**, *111*, 13515−13520.

(36) Tolosa, S.; Sansón, J. A.; Hidalgo, A. *Chem. Phys.* **2008**, *353*, 73−78.

(37) Tolosa, S.; Hidalgo, A.; Sansón, J. A. *J. Phys. Chem. A* **2009**, *113*, 1858−1863.

(38) Tolosa, S.; Hidalgo, A.; Sansón, J. A. *Theor. Chem. Acc.* **2010**, *127*, 671−679.

(39) Tolosa, S.; Hidalgo, A.; Sansón, J. A. *Struc. Chem.* **2011**, *22*, 909−915.

(40) Tolosa, S.; Hidalgo, A.; Sansón, J. A. Neutral hydrolysis of methyl formate from ab initio potentials and molecular dynamics simulation. In *Advances in the Theory of Quantum Systems in Chemistry and Physics*; Hoggan, P. E., Brändas, E. J., Maruani, J., Piecuch, P., Delgado-Barrio, G., Eds.; Springer: Dordrecht, The Netherlands, Heidelberg, Germany, London, and New York, 2012.

(41) Fernández Galván, I.; Martín, M. E.; Aguilar, M. A. *J. Comput. Chem.* **2004**, *25*, 1227−1233.

(42) Wada, G.; Tamura, E.; Okina, M.; Nakamura, M. *Bull. Chem. Soc. Jpn.* **1982**, *55*, 3064−3067.

(43) Haberfield, P. J. *J. Chem. Educ.* **1980**, *57*, 346−346.

(44) Edsall, J. T.; Blanchard, M. H. *J. Am. Chem. Soc.* **1933**, *55*, 2337−2353.

(45) Slifkin, M. A.; Ali, S. M. *J. Mol. Liq.* **1984**, *28*, 215−221.

(46) Nagaoka, M.; Okuyama-Yoshida, N.; Yamabe, T. *J. Phys. Chem. A* **1998**, *102*, 8202−8208.

(47) Tuñón, I.; Silla, E.; Millot, C.; Martins-Costa, M. T. C.; Ruiz-López, M. F. *J. Phys. Chem. A* **1998**, *102*, 8673−8678.

(48) Tortonda, F. R.; Pascual-Ahuir, J. L.; Silla, E.; Tuñón, I. *Chem. Phys. Lett.* **1996**, *260*, 21−26.
(49) Tortonda, F. R.; Pascual-Ahuir, J. L.; Silla, E.; Tuñón, I.; Ramirez, F. J. *J. Chem. Phys.* **1998**, *109*, 592−602.
(50) Tuñon, I.; Silla, E.; Ruiz-Lopez, M. F. *Chem. Phys. Lett.* **2000**, *321*, 433−437.
(51) Rahaman, O.; van Duin, A. C. T.; Goddard, W. A., III; Doren, D. *J. Phys. Chem. B* **2011**, *115*, 249−261.
(52) Balta, B.; Aviyente, V. *J. Comput. Chem.* **2003**, *24*, 1789−1802.
(53) Balta, B.; Aviyente, V. *J. Comput. Chem.* **2004**, *25*, 690−702.
(54) Shoeib, T.; Ruggiero, G. D.; Siu, K. W. M.; Hopkinson, A. C.; Williams, I. H. *J. Chem. Phys.* **2002**, *117*, 2762−2770.
(55) Cui, Q. *J. Chem. Phys.* **2002**, *117*, 4720−4728.
(56) Leung, K.; Rempe, S. B. *J. Chem. Phys.* **2005**, *122*, 184506.
(57) Sambrano, J. R.; de Sousa, A. R.; Queralt, J. J.; Andrés, J.; Longo, E. *Chem. Phys. Lett.* **1998**, *294*, 1−8.
(58) Park, S.-W.; Ahn, D.-S.; Lee, S. *Chem. Phys. Lett.* **2003**, *371*, 74−79.
(59) Gontrani, L.; Mennucci, B.; Tomasi, J. *J. Mol. Struct. (THEOCHEM)* **2000**, *500*, 113−117.
(60) Tortonda, F. R.; Silla, E.; Tuñón, I.; Rinaldi, D.; Ruiz-López, M. F. *Theor. Chem. Acc.* **2000**, *104*, 89−95.
(61) Jeon, I.-S.; Ahn, D.-S.; Park, S.-W.; Lee, S.; Kim, S. K. *Chem. Phys. Lett.* **2005**, *403*, 72−76.
(62) Jeon, I.-S.; Ahn, D.-S.; Park, S.-W.; Lee, S.; Kim, B. *Int. J. Quantum Chem.* **2005**, *101*, 55−66.
(63) Nagy, P. I.; Noszál, B. *J. Phys. Chem. A* **2000**, *104*, 6834−6843.
(64) Kushwaha, P. S.; Mishra, P. C. *J. Mol. Struct. (THEOCHEM)* **2001**, *549*, 229−242.
(65) Carter, E. A.; Hynes, J. T. *J. Phys. Chem.* **1989**, *93*, 2184−2187.
(66) Ando, K.; Hynes, J. T. *J. Phys. Chem. B* **1997**, *101*, 10464−10478.
(67) Ando, K.; Hynes, J. T. *J. Mol. Liq.* **1995**, *64*, 25−37.
(68) Hayashi, S.; Ando, K.; Hynes, J. T. *J. Phys. Chem.* **1995**, *99*, 955−964.
(69) King, G.; Warshel, A. *J. Chem. Phys.* **1990**, *93*, 8682−8692.
(70) Kuharski, R. A.; Bader, J. S.; Chandler, D.; Sprik, M.; Klein, M. L.; Impey, R. W. *J. Chem. Phys.* **1988**, *89*, 3248−3257.
(71) Case, D. A.; Darden, T. A.; Cheatham, I. T. E.; Simmerling, C. L.; Wang, J.; Duke, R. E.; Luo, R.; Mert, K. M.; Wang, B.; Pearlman, D. A. et al., *AMBER 8*; University of California: San Francisco, CA, 2004.
(72) Ewald, P. *Ann. Phys.* **1921**, *64*, 253−287.
(73) Ryckaert, J. P.; Ciccotti, G.; Berendsen, H. J. C. *J. Comput. Phys.* **1977**, *23*, 327−341.
(74) Gaussian 09, Revision A.1, Frisch, M. J.; Trucks, G. W.; Schlegel, H. B.; Scuseria, G. E.; Robb, M. A.; Cheeseman, J. R.; Scalmani, G.; Barone, V.; Mennucci, B.; Petersson, G. A. et al., Gaussian, Inc.: Wallingford CT, 2009.
(75) Refson, K. *Comput. Phys. Commun.* **2000**, *126*, 310−329.
(76) Applegate, K. R.; Slutsky, L. J.; Parker, R. C. *J. Am. Chem. Soc.* **1968**, *90*, 6909−6913.